

# CPEG: Leveraging Consistency Policy with Consensus Guidance for Multi-agent Exploration

Yuqian Fu, *Graduate Student Member, IEEE*, Yuanheng Zhu, *Senior Member, IEEE*, Haoran Li, *Member, IEEE*, Zijie Zhao, *Graduate Student Member, IEEE*, Jiajun Chai, *Graduate Student Member, IEEE*, and Dongbin Zhao, *Fellow, IEEE*

**Abstract**—Efficient exploration is crucial in cooperative multi-agent reinforcement learning (MARL), especially in sparse-reward settings. However, due to the reliance on the unimodal policy, existing methods are prone to falling into the local optima, hindering the effective exploration of better policies. Furthermore, tackling multi-agent tasks in complex environments requires cooperation during exploration, posing substantial challenges for MARL methods. To address these issues, we propose a Consistency Policy with consensus Guidance (CPEG), with two primary components: (a) introducing a multimodal policy to enhance exploration capabilities, and (b) sharing the consensus among agents to foster agent cooperation. For component (a), CPEG incorporates a Consistency model as the policy, leveraging its multimodal nature and stochastic characteristics to facilitate exploration. Regarding component (b), CPEG introduces a Consensus Learner to deduce the consensus on the global state from local observations. This consensus then serves as a guidance for the Consistency Policy, promoting cooperation among agents. The proposed method is evaluated in multi-agent particle environments (MPE) and multi-agent MuJoCo (MAMuJoCo), and empirical results indicate that CPEG not only achieves improvements in sparse-reward settings but also matches the performance of baselines in dense-reward environments.

**Index Terms**—deep reinforcement learning, diffusion model, multi-agent reinforcement learning

## I. INTRODUCTION

RECENT years have witnessed a growing body of applications in cooperative multi-agent reinforcement learning (MARL), such as multi-robot tasks [1] and autonomous driving [2]. Despite these successful applications, cooperative MARL still faces challenges in exploration due to limitations in the policy class regarding multi-modality and the necessity for cooperation in multi-agent systems (MAS) [3].

In single-agent RL, the exploration quality heavily depends on the chosen policy class of agents [4]–[6], with inappropriate policy classes potentially leading to local optima. This issue becomes more pronounced in MARL owing to the complex interaction between agents. In MARL, popular methods [7]–[9] commonly formulate the continuous policy as a unimodal density function, typically a Gaussian distribution. While computationally efficient, these policies can significantly weaken the exploration, as the sampled actions tend to

This work has been submitted to the IEEE for possible publication. Copyright may be transferred without notice, after which this version may no longer be accessible.

The authors are with the State Key Laboratory of Multimodal Artificial Intelligence Systems, Institute of Automation, Chinese Academy of Sciences, Beijing 100190, China, and also with the School of Artificial Intelligence, University of Chinese Academy of Sciences, Beijing 100049, China.

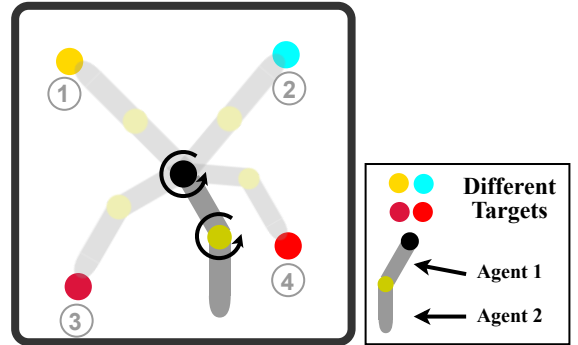


Fig. 1. An example of cooperative exploration. The two-agent arm requires collaborative exploration to reach four targets at different locations. In a sparse reward setting, agents must reach all targets before receiving any reward, making exploration more challenging.

be concentrated around the modality. Besides, the unimodal policy is prone to converging towards a suboptimal policy due to the lack of expressiveness, overfitting the behavior of other agents. To address these challenges, some methods [4], [10], [11] explore alternative policy classes to enhance exploration. Although these methods improve exploration to some extent, they often exhibit limitations in practice. For example, Gaussian mixture models can only cover a limited number of modes, and normalizing flow methods, while able to compute density values, suffer from numerical instability due to their determinant dependence. With the growing prevalence of diffusion models [12], a series of works [13]–[15] apply them as a powerful and multi-modal policy class, primarily in the context of single-agent offline RL. However, the diffusion model is time-intensive, involving multiple sampling steps (*e.g.*, 1000 steps), which makes the training and execution computationally expensive, especially for the online MARL heavily depends on sampling from environments. In order to accelerate the speed of the sampling process, a novel model, the consistency model is designed to map any point at any time step back to the start of the trajectory, based on the probability flow ordinary differential equation (PF-ODE) [12].

Besides, the cooperation among agents during exploration is critical in complex environments [3], [16], [17]. To exemplify, consider the *Reacher4* task depicted in Fig. 1, wherein two agents are required to coordinate their swinging motions to ensure that the end-effector of the manipulator contacts one of the four targets. In a sparse reward setting, agents must

reach all targets before receiving any reward, making exploration more challenging. In this scenario, the agents need to coordinate their actions to set the entire robotic arm in motion, instead of engaging in independent and meaningless actions. Additionally, the agents need to adapt to the multimodality brought by the four targets, avoiding premature convergence to a unimodal policy and achieving simultaneous exploration of multiple targets. This challenge can be tackled through the use of communication-based MARL techniques [18]. However, these techniques introduce challenges such as selecting appropriate information to transmit and additional bandwidth requirements. Recently, some studies [19], [20] leverage a shared *consensus* among agents to promote cooperation. *At each timestep, although the local observations of each agent are unique, they represent different aspects of the same global state.* In the given scenario, observations of the agents only cover their own information such as angular velocity, which serves as partial representations of the global state. However, these individual observations are merely projections of the state. Consequently, our objective is to extract the global state information through consensus, thereby fostering cooperation.

Inspired by the aforementioned observations, we introduce a novel framework tailored to MARL, termed the Consistency Policy with consENSUS Guidance (CPEG), aimed at facilitating efficient cooperative exploration. In this work, we adopt a powerful and effective model, the consistency model as the policy class, with the objective of harnessing its stochastic nature and expressiveness to explore in a multimodal manner. Compared with diffusion models, consistency models enable efficient one-step generation while retaining the advantages of multi-step iterative sampling. For cooperative exploration, we introduce a discrete consensus representation as the guidance for the consistency policy. Specifically, we employ a codebook from VQ-VAE [21] for a discrete, distinguishable consensus representation. This allows agents to derive the same estimation of the global state from a unified consensus codebook, thereby guiding cooperative behaviors. To strike a balance between exploration and exploitation during training, some studies [6], [22] use the mask to decide on exploration or exploitation. Building on the insights from these work, we design a guidance mask to intermittently drop the guidance with probability. Additionally, during the initial phase of training, generative policies may produce unreliable actions, which can affect the training of the policy. To address this, we introduce a self-reference mechanism during the training phase, leveraging past successful experiences to constrain the actions generated by the consistency policy, thus facilitating exploration.

We empirically evaluate the proposed method on two distinct environments: the multiple-particle environment (MPE) [7] and multi-agent MuJoCo (MAMuJoCo) [23]. Across all experiments, we explore both dense-reward settings and sparse-reward settings, where the latter poses significant challenges for exploration as agents receive rewards solely upon completion of a specified task. The results demonstrate that CPEG exhibits notable superiority over competitive baselines in sparse-reward settings and achieves comparable performance in dense-reward settings, thereby underscoring

the effectiveness of our approach.

Our main contributions are summarized as follows:

- 1) We introduce a Consistency Policy for agents, capable of completing the diffusion process in a single step, to explore the environment in a multimodal way. To the best of our knowledge, our study represents the first effort in leveraging consistency policies in MARL.
- 2) We propose a Consensus Learner to infer the global consensus from local observations, aimed at guiding efficient cooperative exploration by sharing the same consensus between agents.
- 3) We incorporate a Self-reference Mechanism to constrain the generated actions by leveraging past successful experiences, thereby reducing the probability of generating invalid actions by policies.
- 4) We evaluate our method on MPE and MAMuJoCo with dense and sparse reward settings. The results indicate that CPEG performs comparably to state-of-the-art (SOTA) algorithms in dense reward environments, while in sparse reward environments, which are more challenging for exploration, our algorithm outperforms SOTA algorithms by 20%.

## II. RELATED WORK

### A. Exploration in MARL

As one of the most critical issues in reinforcement learning, the exploration has drawn great attention in single-agent RL research. This can be even more challenging in complex environments with sparse reward [3]. In the multi-agent domain, several works [16], [17], [24] have emerged to address exploration challenges. MAVEN [24], for instance, aims to maximize the mutual information between the trajectories and latent variables, thereby enabling the learning of diverse exploration policies. EITI and EDTI [16], on the other hand, are designed to capture the influence of one agent's behaviors on others, encouraging agents to visit states that influence the behavior of others. CMAE [17] adopts a shared exploration goal derived from multiple projected state spaces. Beyond these considerations, recent works highlight that the choice of policy class employed by the agents can significantly impact exploration dynamics [4], [5]. However, these efforts primarily concentrate on single-agent domains. In this paper, we highlight the equally crucial role of policy classes in decision-making within multi-agent systems. In our proposed approach, CPEG, we introduce an innovative policy class, the consensus-guided consistency policy, specifically tailored to enhance exploration in MARL.

### B. Diffusion Models for Decision Making

The application of diffusion models in single-agent RL has emerged as a significant trend, showcasing their capability to enhance model expressiveness and improve the decision-making process [25]. Recognized for their powerful and flexible representation, diffusion models find utility in various domains such as trajectory generation [26] and latent skill extraction [27]. Moreover, owing to their exceptional capacity

for representing multimodal distributions, diffusion models are also employed as effective policy classes. In the realm of offline RL, methods like Diffusion-QL [13] and EDP [14] replace conventional Gaussian policies with diffusion models. Building upon the foundational work laid by Janner *et al.* [28], and Wang *et al.* [16], recent studies [29], [30] extend diffusion models to MARL, applying them to trajectory generation and policy estimation. However, it is worth noting that diffusion models typically entail multiple sampling steps, posing a considerable time constraint for diffusion policy methods, particularly in online environments. This challenge is further exacerbated in MARL due to the heightened computational demands as the number of agents increases [31], [32]. To address this issue, some methods adopt faster sampling techniques such as DPM-Solver [33]. Additionally, certain methods like CPQL [34] and Consistency-AC [35] incorporate the consistency model [36], streamlining the sampling process within just one or two diffusion steps. Inspired by these studies, we introduce consistency models as policies into MARL for the first time. Overall, our method not only leverages the multi-modal nature of diffusion models but also significantly enhances the time efficiency.

### III. PRELIMINARIES

#### A. Problem Formulation

We consider a fully cooperative multi-agent task as a *decentralized partially observable Markov decision process* (Dec-POMDP) [37], represented as a tuple  $G = \langle \mathcal{S}, \mathcal{A}, \mathcal{U}, \mathcal{P}, r, \mathcal{O}, \Omega, \gamma \rangle$ , where  $\mathcal{A}$  represents the set of agents with  $|\mathcal{A}| = n_a$ . At each time step, the environment generates the global state  $s \in \mathcal{S}$ , and each agent  $a \in \mathcal{A}$  receives a unique local observation  $o_a \in \mathcal{O}$ , produced by the observation function  $\Omega(s, a) : \mathcal{S} \times \mathcal{A} \rightarrow \mathcal{O}$ . Subsequently, each agent  $a$  selects and executes its own action  $u_a \in \mathcal{U}$ , resulting in a joint action  $\mathbf{u} \in \mathcal{U}^{n_a}$  that induces a state transition according to the state transition function  $\mathcal{P}(s, \mathbf{u}) : \mathcal{S} \times \mathcal{U}^{n_a} \rightarrow \mathcal{S}$ . Meanwhile, the environment provides a global reward shared by all agents, determined by the reward function  $r(s, \mathbf{u}) : \mathcal{S} \times \mathcal{U}^{n_a} \rightarrow \mathbb{R}$ .  $R = \sum_{t=0}^{T_e} \gamma^t r^t$  is the agent's total return, where  $T_e$  denotes the time horizon, and  $\gamma \in [0, 1)$  represents the discount factor.  $Q_a(o, u) = \mathbb{E}_{\{\mathbf{o}_{-a}, \mathbf{u}_{-a}\} \sim \mathcal{B}} [R | o, u, \mathbf{o}_{-a}, \mathbf{u}_{-a}]$  is the action value function for agent  $a$ , where  $\mathbf{o}_{-a}$  and  $\mathbf{u}_{-a}$  denotes the observations and actions of all agents except agent  $a$ . The experience replay buffer  $\mathcal{B}$  contains the tuples  $\langle \mathbf{o}, \mathbf{o}', \mathbf{u}, r \rangle$ .

#### B. Consistency Models

The diffusion model [12] addresses the multimodal distribution matching problem using a stochastic differential equation (SDE), while the consistency model [36] tackles a comparable probability flow ordinary differential equation (PF-ODE):  $dx_\tau/d\tau = -\tau \nabla \log p_\tau(x)$ , where  $\tau \in [0, T]$ ,  $T > 0$  is a fixed constant. Here,  $p_\tau(x) = p_{\text{data}}(x) \otimes \mathcal{N}(0, \tau^2 I)$  denotes the distribution of data  $x_\tau$  at step  $\tau$ , where  $\otimes$  denotes the convolution operation and  $p_{\text{data}}(x) = p_0(x)$  represents the raw data distribution. The reverse process occurs along the solution trajectory  $\{\hat{x}_\tau\}_{\tau \in [\epsilon, T]}$ , with  $\epsilon$  being a small constant close to 0, employed for handling the numerical issues at the

boundary. To accelerate the sampling process of a diffusion model, the consistency model reduces the required number of sampling steps to a significantly smaller value without substantially compromising model generation performance. Specifically, it approximates a parameterized consistency function  $f_\theta : (x_\tau, \tau) \rightarrow x_\epsilon$ , which is defined as a map from the noisy sample  $x_\tau$  at step  $\tau$  back to the original sample  $x_\epsilon$ , in contrast to the step-by-step denoising function  $p_\theta(x_{\tau-1} | x_\tau)$  as the reverse diffusion process in diffusion model. The consistency function possesses the property of self-consistency, meaning its outputs are consistent for arbitrary pairs of  $(x_\tau, \tau)$  that belong to the same PF-ODE trajectory. Besides, for modeling the conditional distribution with condition variable  $c$ , the consistency function is modified to  $f_\theta(c, x_\tau, \tau)$ , representing a slight deviation from the original consistency model.

### IV. METHOD

In this section, we introduce CPEG, a novel approach that integrates the consistency policy guided by consensus between agents for exploration. As illustrated in Fig. 2, our framework consists of three principal components: a) a consistency policy that generates actions from Gaussian noise, b) a discrete consensus representation with masks, which serves as a guidance for cooperation, and c) a self-reference mechanism to constrain consistency policies. Detailed discussions on each component are provided in the subsequent sections.

#### A. Consistency Policy

a) *Notation:* Given the presence of two types of timesteps in this work, one for the diffusion process and one for reinforcement learning, we use superscripts  $\tau \in [0, T]$  to denote diffusion timesteps and subscripts  $t \in \{1, \dots, T_e\}$  to denote environment timesteps.

The consistency policy aims to explore in a multimodal way and avoid falling into local optima. To facilitate understanding, we first formulate the diffusion policy before introducing the consistency policy, which serves as its successor. In diffusion policy, the action of agent  $a$  is diffused with a SDE:

$$du_a^\tau = \mu(u_a^\tau, o_a, \tau) d\tau + \sigma(\tau) dw^\tau, \quad (1)$$

where  $\mu(\cdot, \cdot)$  representing the drift coefficient,  $\sigma(\cdot)$  representing the diffusion coefficient, and  $\{w^\tau\}_{\tau \in [0, T]}$  denoting the standard Brownian Motion. Beginning with  $u_a^T$ , the diffusion policy aims to recover the original action  $u_a^0 = u_a$  by solving a reverse process from  $T$  to 0 using the reverse-time SDE:

$$d\bar{u}_a^\tau = [\mu(u_a^\tau, o_a, \tau) - \sigma(\tau)^2 \nabla \log p_\tau(u_a^\tau, o_a)] d\tau + \sigma(\tau) d\bar{w}^\tau, \quad (2)$$

where  $\bar{w}$  is the reverse Brown Motion, and the score function  $\nabla \log p_\tau(u^\tau)$  is the sole unknown term at each diffusion timestep. Solving the Eq. (2) is challenging in practice, as an alternative, we solve the corresponding PF-ODE:

$$du_a^\tau = \left[ \mu(u_a^\tau, o_a, \tau) - \frac{1}{2} \sigma(\tau)^2 \nabla \log p_\tau(u_a^\tau, o_a) \right] d\tau. \quad (3)$$

Although this diffusion policy can be used for exploration, it is time-intensive and makes the policy inference unacceptably

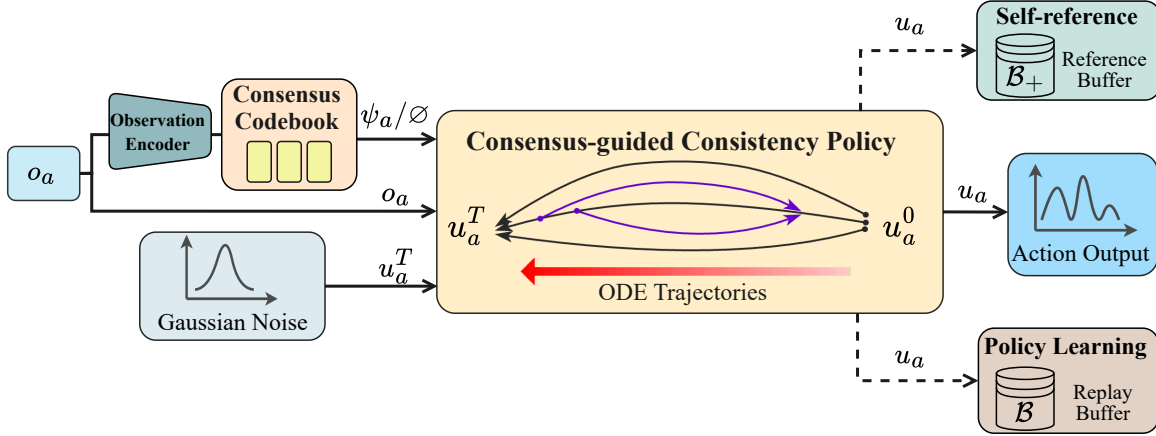


Fig. 2. **The overall framework of the proposed CPEG.** Consensus-guided diffusion policies facilitate cooperative exploration among multiple agents. The consistency policy utilizes the agent’s observation and Gaussian noise as inputs, generating actions under the guidance of masked consensus. The consensus learner consists of an observation encoder, consensus codebook, and state decoder, which learns discrete consensus representations by reconstructing states. During the training phase, in addition to policy learning, the self-reference mechanism provides gradient back-propagation based on the disparity between the agent’s action and those from the reference buffer, thereby imposing a policy constraint.

slow, especially in *tasks that contain multiple agents*. To address this issue, we introduce a consistency policy [34], [36] based on Eq. (3):

$$\begin{aligned} \pi_{\theta_a}(u_a|o_a) &:= f_{\theta_a}(o_a, u_a^{\tau_n}, \tau_n) \\ &= c_{\text{skip}}(\tau_n)u_a^{\tau_n} + c_{\text{out}}(\tau_n)F_{\theta_a}(o_a, u_a^{\tau_n}, \tau_n), \end{aligned} \quad (4)$$

where the initial action  $u_a^{\tau_n} \sim \mathcal{N}(0, \tau_n I)$ , and  $\theta_a$  represents the parameters of the policy  $\pi$  of the agent  $a$ . We discretize the diffusion horizon  $[\epsilon, T]$  into a predetermined sequence  $\{\tau_n | n \in N\}$  of length  $N$  for determining the solution trajectory of action. Moreover,  $\tau_n$  is the  $n$ -th sub-intervals of the time horizon, with  $n \sim \mathcal{U}(1, N - 1)$ . The consistency function  $F_{\theta_a}(o_a, u_a^{\tau_n}, \tau)$  is a trainable deep neural network that accepts the observation  $o_a$  of agent  $a$  as an input and generates an action with dimensions matching  $u_a^{\tau_n}$ .  $c_{\text{skip}}$  and  $c_{\text{out}}$  are differentiable functions, with  $c_{\text{skip}}(\epsilon) = 1$ ,  $c_{\text{out}}(\epsilon) = 0$ , ensuring the consistency process remains differentiable at a fixed, small positive timestep  $\epsilon$ .

In this work, we employ the paradigm of centralized training with decentralized execution (CTDE). Therefore, the joint policy is expressed as a composition of individual policies:

$$\pi_{\theta}(\mathbf{u}|\mathbf{o}) = \prod_{a=1}^{n_a} \pi_{\theta_a}(u_a|o_a). \quad (5)$$

*b) Policy Learning:* To train the consistency policy, we adopt an off-policy optimization approach similar to MADDPG [7]. Following the approach of Wang *et al.* [13], we integrate the Q-value function into the consistency model, training it to preferentially sample actions with higher values:

$$\mathcal{L}_{\text{policy}}(\theta_a) = -\mathbb{E}_{o_a \sim \mathcal{B}, u_a \sim \pi_{\theta_a}(o_a)} [Q(o_a, u_a)]. \quad (6)$$

Specifically, as an estimation of the action value of the agent’s current policy, the parameter  $\beta$  of  $Q(\cdot, \cdot)$  can be learned

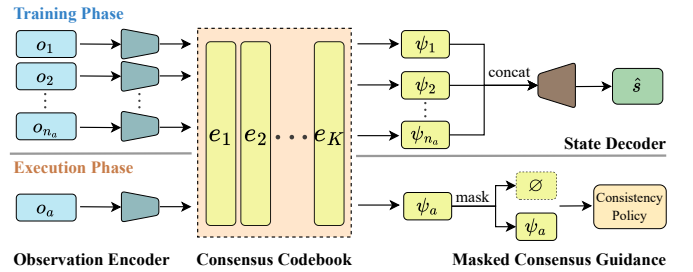


Fig. 3. **The framework of the Consensus Learner.** It operates differently during the training and execution process.

by minimizing the clipped double Q-learning loss [38]:

$$\begin{aligned} \mathcal{L}_{\text{TD}}(\beta_j) &= \mathbb{E}_{\{\mathbf{o}, \mathbf{u}_{-a}\} \sim \mathcal{B}, u_a \sim \pi_{\theta_a}(o_a)} \\ &\left[ \left( (r + \gamma \min_{i \in \{1, 2\}} Q_{\beta_i^{\top}}(\mathbf{o}', u_a') - Q_{\beta_j}(\mathbf{o}, u_a)) \right)^2 \right], j = 1, 2. \end{aligned} \quad (7)$$

where  $\beta, \beta^{\top}$  are the parameter and target parameter of Q-networks respectively.

### B. Consensus Guidance

To guide cooperation in multi-agent exploration, we introduce a consensus learner, where agents sharing the same consensus demonstrate cooperative behaviors. We first formulate a set of  $K$  discrete consensus  $\Psi := \{\psi_1, \dots, \psi_K\}$ , where  $K \in \mathbb{N}$  is a tunable hyperparameter. Each consensus  $\psi_k$  is defined by a tuple  $\langle e_{\psi_k}, I_{\psi_k} \rangle$ , where  $k \in \{1, \dots, K\}$  is the identity of consensus and  $e_{\psi_k} \in \mathbb{R}^m$  is the code (or latent embedding) of consensus  $\psi_k$ .  $I_{\psi_k}$  is the set of agents who have the same consensus  $\psi_k$ , and each agent can only have one consensus at each timestep:  $I_{\psi_i} \cap I_{\psi_j} = \emptyset, \cup_j I_{\psi_j} = I$  for  $i, j \in \{1, 2, \dots, K\}$  and  $i \neq j$ . To represent consensus, we design a consensus learner with VQ-VAE [21], as shown

in Fig. 3. The motivations for this include: a) The discrete codebook in VQ-VAE can effectively extract state features with similar semantics, providing better separation than traditional continuous representation methods. b) The use of discrete feature representation helps mitigate the impact of unavoidable noise on exploration in stochastic environments. c) The discretization process ensures a distinct association, where each agent is linked to a single, specific consensus.

The consensus learner comprises four primary components: an observation encoder, a consensus codebook, a state decoder, and a consensus mask. We assume the consensus can be deduced from the current global state  $s$ . However, for distributed execution in CTDE, each agent  $a$  can only access its local observation  $o_a$ . Considering  $o_a = \Omega(s, a)$  as a projection of the global state  $s$ , we design a two-phase mechanism to deduce consensus from local observations. To deduce the consensus from local observations, the consensus learner has *two modes* during the training and execution phases: during the **training phase**, the consensus learner processes observations from all agents, obtains discrete consensus representations for each agent’s observation, and uses them to reconstruct the global state; in the **execution phase**, it processes agent  $a$ ’s observation to obtain the consensus for guiding policy generation of action  $u_a$ . In this manner, the consensus learner develops the capacity to infer consensus based on local observations.

a) *Observation Encoder*: The encoder  $z_e(\cdot; \alpha_e)$ , parameterized by  $\aleph_e$ , encodes the observation of agent  $o_a$  into an embedding  $z_{e,a} \in \mathbb{R}^m$ , matching the length of the consensus representation  $m$ . In practice, we use historical observations as inputs during each agent’s execution to capture sufficient information about the global state.

b) *Consensus Codebook*: The process of inferring consensus for each input observation proceeds as follows. First, the embedding  $z_{e,a}$  is mapped to a discrete index  $k_a$  of the codebook  $\mathcal{E}$ :

$$k_a = \operatorname{argmin}_{j \in \{1, \dots, K\}} \|z_{e,a} - e_j\|_2, \quad (8)$$

where  $e_j \in \mathcal{E}$  is a codebook vector, and  $K$  denotes the size of the codebook. Notably, the performance of consensus learning is relatively insensitive to the choice of  $K$ , allowing us to set the number of discrete consensus in codebook  $K = 5$  across all scenarios. Based on this discrete index  $k_a$ , the discrete consensus representation for the agent  $a$  is derived as  $\psi_a = e_{k_a}$ . The loss function for the consensus inference process is defined as:

$$\|\operatorname{sg}(z_{e,a}) - e_{k_a}\|_2^2 + \beta \|z_{e,a} - \operatorname{sg}(e_{k_a})\|_2^2, \quad (9)$$

where  $\operatorname{sg}$  denotes the straight-through gradient operation [39], enabling back-propagation training of  $\operatorname{argmin}$  operations, and  $\beta$  is a hyperparameter balancing the degree of alignment between the codebook and input embeddings. In practice, CPEG uses the exponential moving average (EMA) to update the codebook, instead of directly learning them as parameters. Specifically, EMA updates the codebook  $e_{k_a}$  by replacing it with a weighted combination of its previous value  $e_{k_a}$  and the

corresponding vector  $z_{e,a}$ :

$$e_{k_a} \leftarrow \mu z_{e,a} + (1 - \mu) e_{k_a}, \quad (10)$$

where the value of  $\mu$  is a hyperparameter that controls the speed of the moving average updates.

c) *State Decoder*: To develop the ability to deduce consensus from local observations, we aggregate the consensus  $\psi_a$  from all agents together and process them through a state decoder  $z_d(\cdot; \alpha_d)$ , parameterized by  $\alpha_d$ , to reconstruct the global state  $\hat{s}$ . We train the observation encoder and state decoder by maximizing the log-likelihood of the reconstruction:

$$\mathcal{L}_{\text{recon}}(\alpha_{e,d}) = \log p(\hat{s} | z_d(\psi; \alpha_d)), \quad (11)$$

which encourages the encoding and decoding processes of the consensus learner to capture the key information from partial observations for accurate consensus deduction. In addition, the reconstruction loss gradient is also passed to the encoder for training  $\alpha_e$  by straight-through gradient estimation.

d) *Mask Consensus Exploration*: In this work, we employ two distinct exploration strategies: *unguided exploration* and *consensus-guided exploration*, aiming to balance exploration and exploitation to some degree. Unguided exploration allows agents to act according to their current policies without specific consensus guidance, emphasizing their self-directed exploration capabilities. However, its effectiveness is limited by the initial policy quality and the inherent complexities of MAS, neglecting potential cooperative advantages. Considering this, we introduce another exploration strategy, consensus-guided exploration designed to steer the cooperation efforts of agents. The consensus-guided exploration instructs agents to take actions based on the consistency policy guided by their assigned consensus. Through the guidance of shared consensus among different agents, consistency policies can generate cooperative exploration behaviors. Meanwhile, to incorporate consensus guidance, the consistency function  $F_\theta(o, u, \tau)$  in Eq. (4) is modified to  $F_\theta(o, u, \psi, \tau)$ .

To implement the above concept and combine the two exploration mechanisms, we introduce a binary *consensus mask*  $\mathcal{M}$ . This mask can modulate the influence of the consensus vector  $\psi_a$  on action generation by obscuring it through masked attention. We achieve this through masked attention, setting the consensus mask  $\mathcal{M} = 0, \psi_a = \emptyset$  to prevent the downstream generation of  $u_a$  from being guided by the consensus representation. Conversely, when  $\mathcal{M} = 1$ , the consensus representation is incorporated alongside the agent’s observation during action generation. During the **training phase**, the consensus mask  $\mathcal{M}$  is sampled from a Bernoulli distribution with a probability  $p_{\mathcal{M}=1}$ . We set a fixed value  $p_{\mathcal{M}=1} = 0.2$  during training, resulting in a higher proportion of training samples for consensus-guided over unguided exploration. In **execution phase**, we adjust  $p_{\mathcal{M}=1} = 1.0$ , encouraging agents to prioritize consensus-driven actions. It’s noteworthy that a recent work [34] demonstrates that consistency policies can achieve policy improvement with precise guidance. In MARL, given the joint policy’s complexity and the environment’s non-stationarity, precise guidance can more significantly enhance the agents’ policy improvement.

### C. Self-reference Mechanism

Due to the nature of generative models, the consistency policy may generate invalid actions during the initial stages of training [40]. In order to constrain the generated actions, we propose a self-reference mechanism, inspired by self-imitation learning [41]. The self-reference mechanism stores previous experiences in a replay buffer and learns to replicate actions that led to high returns in the past. For each agent, we collect observation-action pairs  $(o_a, u_a)$ , along with their corresponding returns, and store them in the replay buffer  $\mathcal{B}$ . We then sample entries  $(\mathbf{o}, \mathbf{u}, R)$  with empirical returns exceeding the action-value estimates  $Q(\mathbf{o}, u_a)$ , creating a reference buffer  $\mathcal{B}_+ = \{(\mathbf{o}, \mathbf{u}, R) | R \geq Q(\mathbf{o}, u_a)\}$ , where  $u_a$  is generated from the current policy  $\pi_{\theta_a}$ . With  $\mathcal{B}_+$ , the consistency policy of agent  $a$  can be trained with a reference loss function:

$$\mathcal{L}_{\text{ref}}(\theta_a) = \mathbb{E}_{n \sim \mathcal{U}(1, N-1), (o_a, u_a) \sim \mathcal{B}_+} [\lambda(\tau_n) d(f_{\theta_a}(o_a, u_a^{\tau_{n+1}}), \psi_a, \tau_{n+1}), f_{\theta_a^\tau}(o_a, u_a^{\tau_n}, \psi_a, \tau_n)], \quad (12)$$

where  $\lambda(\cdot)$  denotes a step-dependent weight function,  $u^{\tau_n} = u + \tau_n z$ ,  $z \sim \mathcal{N}(0, I)$  and  $d(\cdot, \cdot)$  represents the distance metric. Additionally,  $f_{\theta_a^\tau}$  is the exponential moving average of  $f_{\theta_a}$ , introduced for training stability. The self-reference mechanism in our algorithm offers three benefits: a) As generative methods are prone to generating invalid actions [40], the self-reference mechanism acts as a policy constraint, ensuring more reliable action selection. b) Learning from successful transitions can accelerate exploration during the early training stages. c) self-imitation learning can be viewed as a lower bound of soft Q-learning [42], promoting policy improvement. The pseudocode of CPEG is illustrated in Algorithm 1.

## V. EXPERIMENTS

In this section, we empirically evaluate our method to answer the following questions: (1) Does CPEG effectively contribute to exploration and outperform baselines (See Section V-B, Section V-D)? (2) Can consistency policies alleviate the time-consuming issue associated with diffusion policies (See Section V-C)? (3) How does the consensus learner play a role in cooperative exploration (See Section V-D)? (4) Whether consensus guidance and self-reference mechanism contribute collectively to the final performance (See Section V-E)?

### A. Experimental Settings

a) *Multi-Agent Task Benchmark*: We conduct experiments in two widely-used multi-agent continuous control tasks including the Multi-agent Particle Environments<sup>1</sup> (MPE) [7] and high-dimensional and challenging Multi-Agent MuJoCo<sup>2</sup> (MAMuJoCo) [23] tasks. In MPE, agents known as physical particles need to cooperate to solve various tasks. MAMuJoCo is an extension for MuJoCo locomotion tasks, originally designed for single-agent scenarios, enabling robots to move with the coordination of multiple agents. Specifically, in MPE,

---

### Algorithm 1: Leveraging Consistency Policy with Consensus Guidance for Multi-agent Exploration

---

```

// Initialize
1 Initialize the policy network  $\pi_\theta$  and critic networks  $Q_{\beta_1}, Q_{\beta_2}$ ;
2 Initialize the replay buffer  $\mathcal{B}$  and reference buffer  $\mathcal{B}_+$ ;
3 for episode  $j = 1, \dots, M$  do
4   Reset the environment and receive initial joint observation  $\mathbf{o}$ ;
5   for time step  $t = 1, \dots, H$  do
6     // Consensus guidance
7     For each agent  $a$ , infer consensus  $\psi_a$  by Eq. (8);
8     Sample consensus mask  $\mathcal{M} = \{0, 1\}$ ;
9     Generate  $u_a$  by  $\pi_{\theta_a}$  with consensus  $\psi_a$ , consensus mask  $\mathcal{M}$ , and observation  $o_a$ ;
10    Update consensus learner by Eqs. (9) to (11);
11    // Buffer update
12    Execute actions  $\mathbf{u}$  and observe reward  $r$  and new observation  $\mathbf{o}'$ ;
13    Store  $\langle \mathbf{o}, \mathbf{o}', \mathbf{u}, r \rangle$  in replay buffer  $\mathcal{B}$ ;
14    Update reference buffer  $\mathcal{B}_+$ ;
15    for agent  $a = 1, \dots, n_a$  do
16      // Policy update
17      Sample minibatch  $B \in \mathcal{B}$  and  $B_+ \in \mathcal{B}_+$ ;
18      Update policy  $\pi_{\theta_a}$  by Eq. (6);
19      // Self-reference
20      Constrain policy  $\pi_{\theta_a}$  by self-reference mechanism Eq. (12);
21    end
22    // Q-value update
23    Update Q-value networks  $Q_{\beta_1}, Q_{\beta_2}$  by Eq. (7);
24  end
25 end

```

---

we employ Navigation and Reference as the experimental environments. In MAMuJoCo, the experimental environments include HalfCheetah (2x3), Hopper (3x1), Reacher4 (2x1), and HalfCheetah (6x1).

- **Hopper (3x1)**: This environment features a Hopper in MuJoCo, controlled by agents operating its three primary segments: torso, thigh, and leg. The agents must collaborate effectively to propel the Hopper forward, necessitating intricate coordination as each segment's movement affects the entire structure's balance and progress. In sparse-reward settings, the agent receives a reward only upon advancing a specified distance, which places demands on cooperative exploration.
- **HalfCheetah (2x3) and HalfCheetah (6x1)**: In this environment, the HalfCheetah is a robotic model that resembles a simplified, two-dimensional cheetah. These scenarios involve two and six agents, each representing a front or rear leg. In this shared environment, the agents engage in interactions with the primary objective of advancing forward without falling. These environments parallel the Hopper (3x1) in that agents are rewarded in

<sup>1</sup><https://pettingzoo.farama.org/environments/mpe>

<sup>2</sup>[https://github.com/schroederdewitt/multiagent\\_mujoco](https://github.com/schroederdewitt/multiagent_mujoco)

TABLE I

PERFORMANCE EVALUATION OF RETURNS AND STANDARD DEVIATION IN DIFFERENT SCENARIOS WITH DENSE REWARDS AND SPARSE REWARDS.  $\pm$  CAPTURES THE STANDARD DEVIATION. WE COMPUTED THE AVERAGE SCORES OF EACH ALGORITHM ACROSS DIFFERENT SCENARIOS UNDER TWO SETTINGS. HIGHLIGHTED FIGURES SHOW THE HIGHEST PERFORMANCE AMONG EACH ROW.

Scenarios		CPEG (Ours)	HATD3 [43]	MAPPO [9]	HASAC [43]	MAT [44]	CMAVEN [24]
Dense Reward	Navigation	-68.1±2.0	<b>-66.7±9.1</b>	-84.7±9.7	-68.6±8.3	-66.9±6.8	-88.3±11.2
	Reference	<b>-11.9±1.7</b>	-14.3±4.2	-32.1±3.8	-12.6±2.7	-15.9±2.9	-37.6±4.5
	Reacher4 (2x1)	-22.1±0.4	-22.3±0.8	-22.9±0.5	<b>-21.8±0.2</b>	-23.0±0.2	-26.9±0.3
	HalfCheetah (2x3)	6954.9±466.8	5651.3±441.3	5463.1±392.7	<b>7541.3±472.6</b>	6711.6±459.8	4526.8±314.2
	Hopper (3x1)	3593.4±257.1	3349.9±187.6	3228.3±194.9	<b>3613.2±201.4</b>	2745.8±174.1	2201.4±222.8
	HalfCheetah (6x1)	<b>5692.7±339.4</b>	4782.4±438.6	4083.1±352.1	5535.4±392.4	5057.4±334.7	3343.6±366.2
<b>Average</b>		2689.8±177.9	2279.9±180.3	2105.8±158.9	<b>2764.4±215.4</b>	2401.4±195.7	1983.8±153.2
Sparse Reward	Navigation	<b>19.3±0.3</b>	8.9±1.3	4.2±0.8	10.4±0.6	3.9±0.9	4.9±1.8
	Reference	<b>18.1±0.5</b>	10.4±0.6	3.3±0.8	10.2±0.4	3.8±0.7	8.1±0.9
	Reacher4 (2x1)	<b>50.0±0.0</b>	36.8±0.1	24.4±0.5	38.9±0.6	37.6±0.8	28.5±2.4
	HalfCheetah (2x3)	<b>965.0±8.0</b>	805.0±12.6	703.7±27.9	801.2±10.9	733.7±14.1	629.1±13.2
	Hopper (3x1)	<b>-4.8±0.7</b>	-33.6±3.8	-27.9±2.7	-16.9±0.9	-20.3±4.3	-18.4±3.3
	HalfCheetah (6x1)	<b>704.3±9.8</b>	501.6±10.2	533.6±21.9	622.0±16.4	578.1±18.2	480.7±10.3
<b>Average</b>		<b>291.9±3.8</b>	221.5±4.7	206.8±9.0	244.3±13.9	222.7±6.5	188.7±5.3

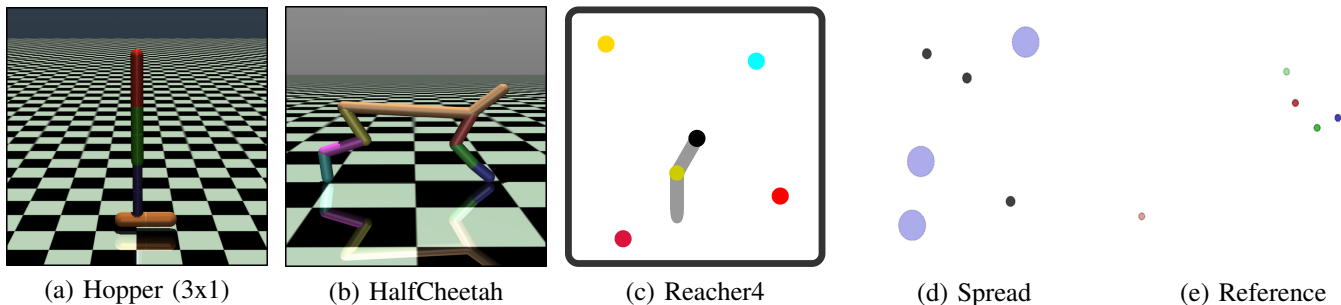


Fig. 4. Demonstrations of five sparse-reward environments. Both HalfCheetah (2x3) and HalfCheetah (6x1) are represented as HalfCheetah.

sparse-reward settings only when they achieve forward movement over a certain distance [45].

- **Reacher4:** To investigate cooperative exploration in a more complex continuous control setting, we propose a two-agent version of the Reacher environment with four targets, Reacher4. The agents are comprised of a two-arm robot, with the goal being to move the robot’s end effector close to one of the four targets. In this scenario, we set up sparse rewards, which means that the agents are rewarded only upon making contact with all four targets.
- **Spread:** In Spread, there are  $n$  agents and  $n$  landmarks. The agents’ goal is to occupy all landmarks. They incur penalties for collisions and are rewarded only when all landmarks are simultaneously covered.
- **Reference:** The Reference scenario requires each agent to approach their designated landmark, which is known only to the other agents. Both agents are simultaneous speakers and listeners. The key challenge lies in the sparsity of the environment’s rewards: agents receive a reward only when all of them reach their designated landmarks simultaneously [46].

Across both environments, we consider dense-reward and

sparse-reward settings, running 2 million steps in MPE and 5 million steps in MAMuJoCo. In the sparse-reward setting, agents don’t receive any intermediate rewards, *i.e.*, agents receive rewards only upon reaching a target or covering a specified distance.

*b) Baselines:* We compared our results with several baselines as follows. HATD3 and HASAC are strong continuous control multi-agent algorithms, which are newly extended from TD3 and SAC by HARL [43]. MAPPO [9] stands as a popular and effective MARL algorithm in the continuous domain, generating actions from Gaussian distribution. MAT [44] addresses the multi-agent challenge as a sequential modeling issue, using the Transformer [47] to generate complex actions. Notably, we observe that few MARL methods focus on exploration within continuous action spaces. Consequently, we extend the classic MARL exploration algorithm MAVEN [24] into its continuous version, termed CMAVEN. Drawing inspiration from FACMAC [23], CMAVEN adopts the cross-entropy method (CEM) — a sampling-based, derivative-free heuristic search strategy—for approximate greedy action selection. CEM has demonstrated effectiveness in identifying near-optimal solutions in nonconvex Q-networks for single-

agent robotic control tasks.

*c) Training Details and Hyper-parameters:* We conduct five independent runs with different random seeds in all scenarios. The experiments in this study were conducted using five distinct seeds on a hardware setup comprising 2 NVIDIA RTX A6000 GPUs and 1 AMD EPYC CPU. We utilized official implementations of baseline algorithms, adhering strictly to their original hyper-parameters. The employed consistency policy involves a multi-layer perceptron (MLP), which processes state inputs to generate corresponding actions. Specifically, our policy networks incorporate a 3-layer MLP architecture with a hidden size of 256, using the Mish activation function. The consensus learner consists of a MLP, a consensus codebook module, and another MLP. The MLP network is a 128-dimensional fully-connected layer, followed by a GELU activation, and followed by another 128-dimensional fully-connected layer.

For the consistency policy, we define the diffusion step  $k$  within the range of  $[0.002, 80.0]$ , setting the number of sub-intervals  $M = 40$ . Following Karras diffusion model, the sub-interval boundaries are determined with the formula  $k_i = \left( \epsilon^{\frac{1}{\rho}} + \frac{i-1}{M-1} \left( T^{\frac{1}{\rho}} - \epsilon^{\frac{1}{\rho}} \right) \right)^\rho$ , where  $\rho = 7$ . The Euler method is employed as the ODE solver. In the consensus learner, we set the number of discrete consensus in codebook  $K = 5$  in different scenarios, and  $\beta = 0.2$ . The performance of consensus learning is not sensitive to the setting of  $K$ . Regarding performance evaluation, we pause training every  $M$  steps and evaluate for  $N$  episodes with action selection. The  $(M, N)$  in MPE and MAMuJoCo are  $(1000, 20)$  and  $(10000, 40)$ , respectively. The training objective is optimized by Adam with a learning rate of  $5 \times 10^{-4}$ .

## B. Performance Comparison

We first compare CPEG with baselines across six scenarios. Table I outlines the comparison between our approach and various baseline algorithms in both dense reward and sparse reward settings. In *dense-reward* environments, CPEG demonstrates performance slightly below or comparable to baselines, surpassing them in specific tasks. In the context of online MARL in POMDPs, the theoretically optimal policy tends to be deterministic, suggesting that expressive models often revert to unimodal to approach optimality. Consequently, expressiveness primarily aids in exploration rather than contributes to the final optimal policy convergence. In *sparse-reward* environments requiring exploration, CPEG approach exhibits a significant performance advantage, outperforming baseline algorithms by 20%. While methods like HATD3, MAPPO, and MAT show proficiency in dense reward contexts, their limited focus on exploration hinders their effectiveness in reaching sparse reward states. Although the HASAC method improves exploration capability through entropy regularization, the disparity between its employed Gaussian policy and the assumed theoretical Boltzmann policy leads to local optima, thereby constraining exploration. Notably, despite being tailored for MARL exploration, CMAVEN struggles considerably in continuous action spaces, resulting in underwhelming performance. In contrast, our proposed method, employing

the consistency policy with consensus guidance and a self-inference mechanism, fosters more efficient exploration and significantly enhances performance.

## C. Time Efficiency

In addition to its superior performance, CPEG also possesses higher time efficiency compared with methods based on diffusion models. This efficiency is essential for practical scalability in multi-agent systems and for facilitating real-time decision-making processes. To demonstrate this, we replace the policy class in our method with a diffusion model (CPEG-DM) and an accelerated variant of it (CPEG-DPM) [33], and compared the time required by the different algorithms for each training iteration, as shown in Table II.

In Navigation and HalfCheetah(2x3) scenarios, our method attains training speeds up to  $6.6\times$  and  $6.8\times$  faster than those of diffusion-based methods, rivaling the time efficiency of previous methods like HATD3. Despite using DPM-Solver, CPEG-DPM still faces challenges in achieving satisfactory training efficiency. Moreover, the training speed of algorithms is greatly impacted by the scaling in MAS. We selected Humanoid(17x1) scenario, which involves 17 agents, for evaluating our methods under large-scale agents. In this scenario, the training time of diffusion-based methods significantly exceeds that of CPEG, demonstrating the scalability of our method in MARL.

Due to the substantial reduction in sampling steps, the consistency model is inherently less expressive than the diffusion model [36]. To evaluate this, we conduct a performance comparison between CPEG and diffusion-based methods in three sparse scenarios. In comparison to CPEG-DM and CPEG-DPM, CPEG exhibits a performance decrease in MPE scenarios, yet outperforms it in the HalfCheetah(2x3) and Humanoid(17x1) environments. This phenomenon could potentially be attributed to that the consistency policy can effectively transmit action gradients in one step, thereby alleviating the challenges of policy training via Q-function in diffusion-based methods [34]. Moreover, the slight performance trade-off in CPEG is considered acceptable, given its significant improvements in training and online inference efficiency.

## D. Qualitative Analysis and Visualization

To showcase the exploration capabilities of our method, consider a didactic example illustrated in Fig. 5(a), which demonstrates different MARL algorithms applied to the sparse Reacher4 task [23] featuring four targets. The agents consist of two-arm robots tasked with moving the robot's end effector close to one of the four targets. The depth of color represents the magnitude of the state visitation probability. In this scenario, we configure sparse rewards, meaning that the agents receive rewards only upon making contact with all four targets. Besides, the agents need to cooperate in exploration to reach the target, and the dispersion of targets often leads to agents adopting one single policy, underscoring the necessity for multimodal policies and cooperative exploration. In Fig. 5(b), our method learns a multimodal joint



TABLE II  
**PERFORMANCE (HIGHER IS BETTER) AND TIME EFFICIENCY (LOWER IS BETTER) COMPARISON.** WE COMPARE CPEG, HATD3, AND DIFFUSION-BASED METHODS IN THREE SPARSE-REWARD SCENARIOS, WHERE TIME DENOTES THE DURATION OF A SINGLE ITERATION.

Scenarios	Performance $\uparrow$				Time (ms) $\downarrow$			
	HATD3	CPEG	CPEG-DM	CPEG-DPM	HATD3	CPEG	CPEG-DM	CPEG-DPM
Navigation	8.9 $\pm$ 1.3	19.3 $\pm$ 0.3	<b>25.9<math>\pm</math>1.8</b>	20.5 $\pm$ 1.1	<b>21</b>	48	316	166
HalfCheetah (2x3)	805.0 $\pm$ 12.6	<b>965.0<math>\pm</math>8.0</b>	943.6 $\pm$ 7.2	914.3 $\pm$ 7.4	<b>12</b>	37	247	129
Humanoid (17x1)	902.8 $\pm$ 4.7	<b>1143.6<math>\pm</math>9.1</b>	991.5 $\pm$ 8.4	878.9 $\pm$ 9.5	<b>155</b>	249	2133	1645

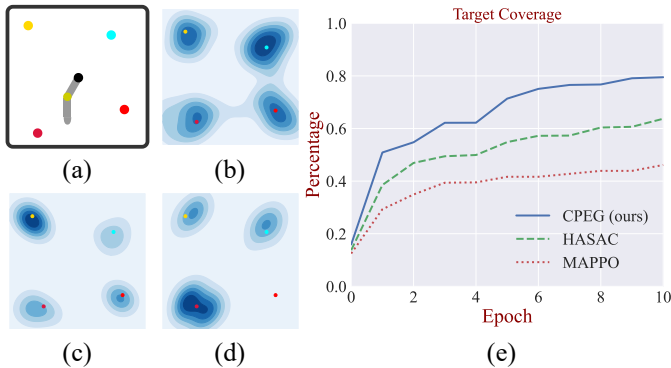


Fig. 5. **Example results obtained by CPEG and baselines on exploration visitation.** (a) shows a Reacher4 task, with four targets in different colors. (b)-(d) shows the state visitation of CPEG, HASAC and MAPPO. (e) counts the targets covered by policies during exploration.

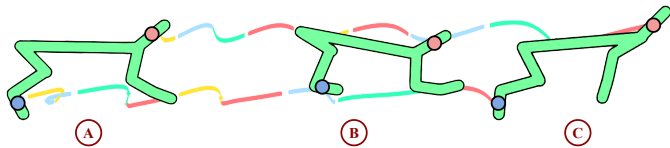


Fig. 6. **Trajectory visualization in HalfCheetah (2x3).** Different colors represent the corresponding consensus between agents.

policy, enabling the effector to reach four different targets relatively uniformly, without converging to a unimodal policy. Conversely, in Fig. 5(c) and (d), baselines primarily focus on visiting certain targets, thereby limiting exploration in the complex environment. Additionally, we quantify the targets covered by the policy during exploration in Fig. 5(e). The curves indicate that our method achieves a state visitation rate of 83%, compared to 62% for HASAC, reflecting a 20% improvement. These results demonstrate that CPEG can facilitate a more efficient exploration of the four different targets in the scenario, highlighting the importance of multimodal policies and cooperative exploration capabilities among agents.

In order to gain a better understanding of the consensus learner within CPEG, we generate visualizations of consensus guidance and observation embeddings. In Fig. 6, we visualize the *true* trajectories generated by the consensus-guided consistency policy in the HalfCheetah(2x3) scenario. The trajectories are color-coded to represent the corresponding consensus generated during execution. Across stages A, B, and C, although the observations of the two agents differ,

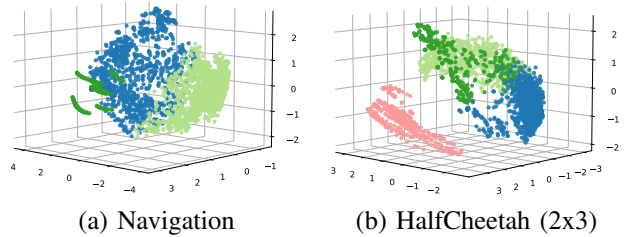


Fig. 7. **Visualization of the observation embeddings.** We choose the last 30k steps for visualization. The colors denote different consensus.

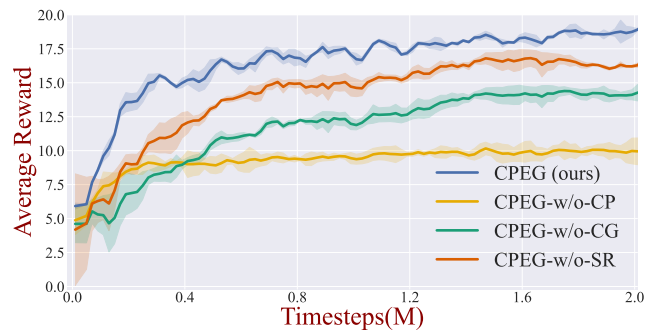


Fig. 8. The ablation performance of the three key components in our method under the sparse Navigation scenario.

they converge to a common consensus (the same color). This indicates that the consensus effectively reflects the global state, enabling multiple agents to coordinate their actions. By leveraging this shared consensus, multiple agents can cooperate more effectively, thereby enhancing their exploration of the environment. Additionally, we present the visualizations obtained by applying the PCA technique to the observation embeddings. The goal is to show whether the consensus learner can deduce distinguishable consensus from the local observations, aiding in the guidance of policy during the exploration process. As shown in Fig. 7, the visualizations demonstrate that the consensus learner can generate informative discrete representations by identifying potential correlations within individual observations of agents.

### E. Ablation Study

In this subsection, we conduct ablation studies in Navigation scenario to investigate the impact of three main components in CPEG: (1) replacing the consistency policy with a deterministic policy (similar to MADDPG), while

incorporating consensus guidances and observations directly as the inputs (*CPEG-w/o-CP*), (2) removing the consensus learner module, forcing agents to rely solely on their own observations for exploration during training (unguided exploration) and achieving objectives during execution (*CPEG-w/o-CG*), and (3) removing the self-reference mechanism, which relaxes the constraint on consistency policies (*CPEG-w/o-SR*). The experimental results, as shown in Fig. 8, reveal that *CPEG-w/o-CP* quickly converges to a locally optimal policy. This result indicates that the consistency policy significantly enhances the exploration, preventing agents from converging to local optima. Additionally, CPEG outperforms *CPEG-w/o-CG*, which does not use consensus guidance, in both convergence rate and final performance. Similarly, when using only consensus guidance, *CPEG-w/o-SR* exhibits a lack of exploitation of past successes, reducing sample efficiency and leading to performance degradation. Overall, the results indicate that these elements collectively contribute to the improved performance of our method.

## VI. CONCLUSIONS AND FUTURE WORK

In this paper, we propose CPEG, a novel multi-agent exploration method with a consensus-guided consistency policy that facilitates cooperative exploration and a self-reference mechanism that constrains the generated actions. To the best of our knowledge, our study represents the first effort in leveraging consistency policies in MARL. The empirical results from six environments demonstrate that CPEG performs comparably to baseline algorithms in dense reward settings while in sparse reward settings, which pose more challenges for exploration, our algorithm outperforms baselines by 20%.

This work is the first to showcase the advantages of consensus-guided consistency policies in the realm of multi-agent exploration. On the other hand, the present work is confined to exploration within single-task scenarios. In the future, we intend to study how to better harness the multimodal nature of consistency policies to devise a faster and more efficient algorithm for multi-task MARL.

## REFERENCES

- [1] G. Hu, H. Li, S. Liu, Y. Zhu, and D. Zhao, "NeuronsMAE: a novel multi-agent reinforcement learning environment for cooperative and competitive multi-robot tasks," in *International Joint Conference on Neural Networks*. IEEE, 2023, pp. 1–8.
- [2] Q. Zhang, Y. Gao, Y. Zhang, Y. Guo, D. Ding, Y. Wang, P. Sun, and D. Zhao, "Trajgen: Generating realistic and diverse trajectories with reactive and feasible agent behaviors for autonomous driving," *IEEE Transactions on Intelligent Transportation Systems*, vol. 23, no. 12, pp. 24 474–24 487, 2022.
- [3] J. Hao, T. Yang, H. Tang, C. Bai, J. Liu, Z. Meng, P. Liu, and Z. Wang, "Exploration in deep reinforcement learning: From single-agent to multiagent domain," *IEEE Transactions on Neural Networks and Learning Systems*, pp. 1–21, 2023.
- [4] B. Mazouze, T. Doan, A. Durand, J. Pineau, and R. D. Hjelm, "Leveraging exploration in off-policy algorithms via normalizing flows," in *Conference on Robot Learning*, 2020.
- [5] Z. Huang, L. Liang, Z. Ling, X. Li, C. Gan, and H. Su, "Reparameterized policy learning for multimodal trajectory optimization," in *International Conference on Machine Learning*, 2023.
- [6] A. Sridhar, D. Shah, C. Glossop, and S. Levine, "NoMaD: Goal masked diffusion policies for navigation and exploration," in *NeurIPS 2023 Foundation Models for Decision Making Workshop*, 2023.
- [7] R. Lowe, Y. I. Wu, A. Tamar, J. Harb, O. Pieter Abbeel, and I. Mordatch, "Multi-agent actor-critic for mixed cooperative-competitive environments," in *Advances in Neural Information Processing Systems*, 2017.
- [8] J. G. Kuba, R. Chen, M. Wen, Y. Wen, F. Sun, J. Wang, and Y. Yang, "Trust region policy optimisation in multi-agent reinforcement learning," in *International Conference on Learning Representations*, 2022.
- [9] C. Yu, A. Velu, E. Vinitzky, J. Gao, Y. Wang, A. Bayen, and Y. Wu, "The surprising effectiveness of PPO in cooperative multi-agent games," in *Thirty-sixth Conference on Neural Information Processing Systems Datasets and Benchmarks Track*, 2022.
- [10] A. Kumar, J. Fu, M. Soh, G. Tucker, and S. Levine, "Stabilizing off-policy q-learning via bootstrapping error reduction," in *Advances in Neural Information Processing Systems*, 2019.
- [11] J. Ren, Y. Li, Z. Ding, W. Pan, and H. Dong, "Probabilistic mixture-of-experts for efficient deep reinforcement learning," *arXiv preprint arXiv: 2104.09122*, 2021.
- [12] Y. Song, J. Sohl-Dickstein, D. P. Kingma, A. Kumar, S. Ermon, and B. Poole, "Score-based generative modeling through stochastic differential equations," in *International Conference on Learning Representations*, 2021.
- [13] Z. Wang, J. J. Hunt, and M. Zhou, "Diffusion policies as an expressive policy class for offline reinforcement learning," in *International Conference on Learning Representations*, 2023.
- [14] B. Kang, X. Ma, C. Du, T. Pang, and S. Yan, "Efficient diffusion policies for offline reinforcement learning," in *Advances in Neural Information Processing Systems*, 2023.
- [15] H. Li, Y. Zhang, H. Wen, Y. Zhu, and D. Zhao, "Stabilizing diffusion model for robotic control with dynamic programming and transition feasibility," *IEEE Transactions on Artificial Intelligence*, vol. 1, no. 01, pp. 1–11, 2024.
- [16] T. Wang, J. Wang, Y. Wu, and C. Zhang, "Influence-based multi-agent exploration," in *International Conference on Learning Representations*, 2020.
- [17] I.-J. Liu, U. Jain, R. A. Yeh, and A. Schwing, "Cooperative exploration for multi-agent deep reinforcement learning," in *International Conference on Machine Learning*, 2021.
- [18] G. Hu, Y. Zhu, D. Zhao, M. Zhao, and J. Hao, "Event-triggered communication network with limited-bandwidth constraint for multi-agent reinforcement learning," *IEEE Transactions on Neural Networks and Learning Systems*, vol. 34, no. 8, pp. 3966–3978, 2023.
- [19] Z. Xu, B. Zhang, D. Li, Z. Zhang, G. Zhou, and G. Fan, "Consensus learning for cooperative multi-agent reinforcement learning," in *AAAI Conference on Artificial Intelligence*, 2022.
- [20] J. Ruan, X. Hao, D. Li, and H. Mao, "Learning to collaborate by grouping: A consensus-oriented strategy for multi-agent reinforcement learning," in *European Conference on Artificial Intelligence*, 2023.
- [21] A. Van Den Oord, O. Vinyals *et al.*, "Neural discrete representation learning," in *Advances in Neural Information Processing Systems*, 2017.
- [22] V. Zangirolami and M. Borrotti, "Dealing with uncertainty: Balancing exploration and exploitation in deep recurrent reinforcement learning," *Knowledge-Based Systems*, vol. 293, p. 111663, 2024.
- [23] B. Peng, T. Rashid, C. Schroeder de Witt, P.-A. Kamienny, P. Torr, W. Böhrer, and S. Whiteson, "FACMAC: Factored multi-agent centralised policy gradients," in *Advances in Neural Information Processing Systems*, 2021.
- [24] A. Mahajan, T. Rashid, M. Samvelyan, and S. Whiteson, "MAVEN: Multi-agent variational exploration," *Advances in Neural Information Processing Systems*, 2019.
- [25] Z. Zhu, H. Zhao, H. He, Y. Zhong, S. Zhang, Y. Yu, and W. Zhang, "Diffusion models for reinforcement learning: A survey," *arXiv preprint arXiv:2311.01223*, 2023.
- [26] A. Ajay, Y. Du, A. Gupta, J. B. Tenenbaum, T. S. Jaakkola, and P. Agrawal, "Is conditional generative modeling all you need for decision making?" in *International Conference on Learning Representations*, 2023.
- [27] S. Venkatraman, S. Khaitan, R. T. Akella, J. Dolan, J. Schneider, and G. Berseth, "Reasoning with latent diffusion in offline reinforcement learning," in *International Conference on Learning Representations*, 2024.
- [28] M. Janner, Y. Du, J. Tenenbaum, and S. Levine, "Planning with diffusion for flexible behavior synthesis," in *International Conference on Machine Learning*, 2022.
- [29] Z. Zhu, M. Liu, L. Mao, B. Kang, M. Xu, Y. Yu, S. Ermon, and W. Zhang, "MADiff: Offline multi-agent learning with diffusion models," *arXiv preprint arXiv: 2305.17330*, 2023.

- [30] Z. Li, L. Pan, and L. Huang, “Beyond conservatism: Diffusion policies in offline multi-agent reinforcement learning,” *arXiv preprint arXiv:2307.01472*, 2023.
- [31] J. Chai, Y. Zhu, and D. Zhao, “NVIF: Neighboring variational information flow for cooperative large-scale multiagent reinforcement learning,” *IEEE Transactions on Neural Networks and Learning Systems*, pp. 1–13, 2023.
- [32] J. Chai, Y. Fu, D. Zhao, and Y. Zhu, “Aligning credit for multi-agent cooperation via model-based counterfactual imagination,” in *International Conference on Autonomous Agents and Multiagent Systems*, 2024, pp. 281–289.
- [33] C. Lu, Y. Zhou, F. Bao, J. Chen, C. Li, and J. Zhu, “DPM-solver: A fast ODE solver for diffusion probabilistic model sampling in around 10 steps,” in *Advances in Neural Information Processing Systems*, 2022.
- [34] Y. Chen, H. Li, and D. Zhao, “Boosting continuous control with consistency policy,” in *International Conference on Autonomous Agents and Multiagent Systems*, 2024.
- [35] Z. Ding and C. Jin, “Consistency models as a rich and efficient policy class for reinforcement learning,” in *International Conference on Learning Representations*, 2024.
- [36] Y. Song, P. Dhariwal, M. Chen, and I. Sutskever, “Consistency models,” in *International Conference on Machine Learning*, 2023.
- [37] F. A. Oliehoek, C. Amato *et al.*, *A concise introduction to decentralized POMDPs*. Springer, 2016, vol. 1.
- [38] S. Fujimoto, H. Hoof, and D. Meger, “Addressing function approximation error in actor-critic methods,” in *International Conference on Machine Learning*, 2018.
- [39] Y. Bengio, N. Léonard, and A. Courville, “Estimating or propagating gradients through stochastic neurons for conditional computation,” *arXiv preprint arXiv:1308.3432*, 2013.
- [40] C. Chen, R. Karunasena, T. H. Nguyen, A. Sinha, and P. Varakantham, “Generative modelling of stochastic actions with arbitrary constraints in reinforcement learning,” in *Advances in Neural Information Processing Systems*, 2023.
- [41] J. Oh, Y. Guo, S. Singh, and H. Lee, “Self-imitation learning,” in *International Conference on Machine Learning*, 2018.
- [42] Y. Tang, “Self-imitation learning via generalized lower bound q-learning,” in *Advances in Neural Information Processing Systems*, 2020.
- [43] Y. Zhong, J. G. Kuba, X. Feng, S. Hu, J. Ji, and Y. Yang, “Heterogeneous-agent reinforcement learning,” *Journal of Machine Learning Research*, vol. 25, no. 32, pp. 1–67, 2024.
- [44] M. Wen, J. G. Kuba, R. Lin, W. Zhang, Y. Wen, J. Wang, and Y. Yang, “Multi-agent reinforcement learning is a sequence modeling problem,” in *Advances in Neural Information Processing Systems*, 2022.
- [45] Y. Guo, J. Choi, M. Moczulski, S. Feng, S. Bengio, M. Norouzi, and H. Lee, “Memory based trajectory-conditioned policies for learning from sparse rewards,” in *Advances in Neural Information Processing Systems*, 2020.
- [46] Z. Zhang, Y. Liang, Y. Wu, and F. Fang, “MESA: Cooperative meta-exploration in multi-agent learning through exploiting state-action space structure,” in *International Conference on Autonomous Agents and Multiagent Systems*, 2024, pp. 2085–2093.
- [47] A. Vaswani, N. M. Shazeer, N. Parmar, J. Uszkoreit, L. Jones, A. N. Gomez, L. Kaiser, and I. Polosukhin, “Attention is all you need,” in *Advances in Neural Information Processing Systems*, 2017.